Numerical implementation of the wave-turbulence closure of turbulence in a rotating channel

Aleksandr Eremin, Julian F. Scott, Fabien Godeferd, Anne Cadiou

Numerical implementation of the wave-turbulence closure of turbulence in a rotating channel

A. EREMIN, J.F. SCOTT, F.S. GODEFERD, A. CADIOU

Laboratoire de Mécanique des Fluides et d'Acoustique (LMFA)
UMR 5509 CNRS — Université de Lyon
Université Claude Bernard, Ecole Centrale de Lyon, INSA - Lyon, France
aleksandr.eremin@doctorant.ec-lyon.fr, julian.scott@ec-lyon.fr

Résumé :

Nous utilisons une fermeture de turbulence d'ondes pour étudier la turbulence en rotation rapide en décroissance libre, confinée dans la direction de l'axe de rotation entre deux parois planes parallèles (Scott, 2014). Le confinement résulte en la dicrétisation des modes du mouvement fluide dans cette direction, alors que l'écoulement est supposé statistiquement homogène dans les autres directions. Le modèle de turbulence d'ondes est implémenté numériquement, et nous étudions ici sa convergence, précision et efficacité parallèle. Les résultats présentés portent sur l'effet de l'amortissement de paroi et de la dissipation sur la dynamique, sur l'évolution de l'énergie cinétique, et sur la distribution de l'énergie entre les modes.

Abstract :

Wave-turbulence closure is used to study rapidly rotating decaying turbulence confined in a single direction of the rotation axis, between two plane parallel walls (Scott, 2014). The confinement leads to the discretization of the modes in this direction, whereas the flow is assumed to be statistically homogeneous in unconfined directions. The wave-turbulent closure is numerically implemented, and we study here its convergence, accuracy and parallel efficiency. Results concern the effect of wall damping and volumetric dissipation on the dynamics, the evolution of kinetic energy, and the energy distribution between modes.

Keywords: Confined Turbulence, Rotating Turbulence, Wave-Turbulence, Statistical Closure

1 Introduction

Turbulence is often subjected to the influence of rotation in many applications such as meteorology, ocean dynamics and astrophysics. Capturing this effect in models for rotating turbulent flows is important for the accurate description of the dynamics related to the presence of the inertial waves, which interact and lead to wave-turbulence dynamics [5]. Anisotropy is an important feature of these flows. Multiscale models, such as the Eddy-Damped Quasi-Normal Markovian one (EDQNM) [3, 4], have

been specifically adapted for including rotation, and are consistent with wave-turbulence theory. Being spectral, they assume statistical homogeneity of turbulence. However, turbulence is never really unbounded and homogeneous and the effects of confinement and the consequent lack of homogeneity are usually important. In this study, we propose a numerical implementation for the new wave-turbulence statistical model for confined rotating turbulence developed by Scott (2014) [6].

In the following, we present the salient features of the wave-turbulence model in Section 2, the numerical resolution of the model and the analysis of convergence with respect to numerical parameters (Section 3), our first results about the dynamics (Section 4), and conclusions and perspectives (Section 5).

2 Wave-turbulence closure

2.1 Governing equation

We study decaying turbulence confined between two infinite parallel walls that rapidly rotate about an axis perpendicular to them. The turbulence is assumed to be statistically homogeneous [1] in unconfined directions parallel to the walls, but confinement means that it is inhomogeneous with respect to the third direction. We consider the velocity field as a combination of inviscid linear inertial waveguide modes. These modes are parameterized by a real wave vector $\boldsymbol{k} = (k_1, k_2)$ in the homogeneous directions x_1, x_2 and by an integer number n in the confinement direction x_3, denoting the waveguide mode which is considered.

The flow can be separated into a three-dimensional wave-turbulence part, and a two-dimensional (2D) part containing non-dispersive $n = 0$ modes. Their superposition represents a steady 2D flow ($u_3 = 0, u_1 = u_1(x_1, x_2), u_2 = u_2(x_1, x_2)$), which is decoupled from the wave component of turbulence.

The statistical charaterization of wave-turbulence uses two-point velocity correlations which are represented by the spectral matrix $A_{nm}(k, t)$, where $k = |\boldsymbol{k}|$. This matrix is defined via the statistical average of products of the amplitudes of modes of orders n and m. The diagonal elements ($n = m$) of this matrix are therefore real and positive. They represent the distribution of energy over the modes n and horizontal wavenumber k. The off-diagonal elements can be complex and express correlations between modes of different orders. Our aim is to study the time evolution of $A_{nm}(k, t)$ in limits of small Rossby number ε.

As expected for wave turbulence, energy transfer between wave modes occurs in resonant triads and takes place at times $O(\varepsilon^{-2})$ multiples of the rotational period. In the limit of small Rossby number, nonlinear effects are small and, in order that viscous dissipation not kill the turbulence before nonlinearity becomes significant, the Ekman number E must also be small. When both numbers are small, it is found that viscosity leads to a linear damping term in the amplitude equations.

The governing equation of this model is

$$\frac{\partial A_{nn}(k)}{\partial t} + 2\mathrm{Re}(\Delta_\mathrm{n}(\mathrm{k}))\mathrm{A}_\mathrm{nn}(\mathrm{k}) = \sum_{n_p,\ n_q \neq 0} \oint_{C_{nn_pn_q}(\boldsymbol{k})} \frac{A_{n_pn_p}(p)\left(\eta_{nn_pn_q}(\boldsymbol{k},\boldsymbol{p})A_{nn}(k) + \lambda_{nn_pn_q}(\boldsymbol{k},\boldsymbol{p})A_{n_qn_q}\left(|\boldsymbol{k}+\boldsymbol{p}|\right)\right)}{\Gamma_{n_pn_q}(\boldsymbol{k},\boldsymbol{p})} |\mathrm{d}\boldsymbol{p}| \quad (1)$$

where Re denotes the real part of a complex number and $n \neq 0$. The damping factor $\Delta_n(k)$ is the sum of two terms representing damping by Ekman pumping by the wall boundary layers of $O(E^{1/2})$

and dissipation from outside the layers of $O(E)$. The curve integral is taken over the resonance curve $C_{nn_pn_q}(\boldsymbol{k})$ which is the locus of points in the $\boldsymbol{p}$ plane for which the resonance condition is satisfied:

$$\sigma_{nn_pn_q}(\boldsymbol{k},\boldsymbol{p}) \stackrel{\text{def}}{=} \omega_n(k) + \omega_{n_p}(p) + \omega_{n_q}(|\boldsymbol{k}+\boldsymbol{p}|) = 0, \tag{2}$$

where

$$\omega_n(k) = \frac{n\pi}{(k^2+n^2\pi^2)^{1/2}}$$

is the dispersion relation for inertial wave modes. If Eq. (2) has no solutions, integrals should be interpreted as zero.

In Eq. (1), $\Gamma_{n_pn_q}(\boldsymbol{k},\boldsymbol{p})$ is defined as

$$\Gamma_{n_pn_q}(\boldsymbol{k},\boldsymbol{p}) = \frac{1}{\pi}\left|\nabla_{\boldsymbol{p}}\sigma_{nn_pn_q}(\boldsymbol{k},\boldsymbol{p})\right|$$

and $\eta_{nn_pn_q}(\boldsymbol{k},\boldsymbol{p})$ and $\lambda_{nn_pn_q}(\boldsymbol{k},\boldsymbol{p})$ are zero unless one of the four conditions $n \pm n_p \pm n_q = 0$ is met. This, along with $\boldsymbol{k}+\boldsymbol{p}+\boldsymbol{q}=0$, are the conditions for mode-triad nonlinear coupling. It has been shown that the two-dimensional component has no influence on the evolution of A_{nn} for $n \neq 0$, therefore sum indices in Eq. (1) ignore zero values. However, the two-dimensional component has an impact on the off-diagonal elements of the matrix A_{nm}, making it decay on a time scale ε^{-1}. Finally, Eq. (1) is a closed evolution equation of the wave energy spectrum.

In what follows, we denote diagonal elements as $B_n(k) = \varepsilon^{-2}A_{nn}(k)$ and time $T = \varepsilon^2 t$, of $O(1)$. The initial form of the spectrum is chosen as

$$B_n(k) = \alpha e^{\frac{-(k^2+n^2\pi^2)}{\Xi^2}} \tag{3}$$

where Ξ is the spectral width and α is a constant such that

$$2\pi\sum_{n=1}^{\infty}\int_0^{\infty} kB_n(k,t)\mathrm{d}k = 1.$$

It follows that the wave-component part of the energy is initially equal to ε^2.

2.2 Critical points

As mentioned above, the resonance curve defined by Eq. (2) does not always have a solution. Moreover, it can be shown that if the resonance curve $C_{nn_pn_q}(\boldsymbol{k})$ exists, it consists only of a single loop (unlike the multiple-branched resonance surfaces for inertial waves in three-dimensional homogeneour rotating turbulence [2]). For $n_p, n_q < 0$ it always exists, but for n_p and n_q of different signs it exists only for large enough k, and as k decreases through a certain wavenumber k_c the resonance curve disappears via a small ellipse and does not give contributions to the right-hand side of Eq. (1). The wavenumber k_c can be characterized as a point where the change of loop can occur. This amounts to satisfying both the resonance condition Eq. (2) and

$$\nabla\sigma_{nn_pn_q}(k,\boldsymbol{p}) = 0\,. \tag{4}$$

The wavenumbers k_c together with $\boldsymbol{p_c}$ are referred to as critical points, $k_c, \boldsymbol{p_c}$. Physically, they correspond to wave-vector triads at which the dispersivity of the wave system vanishes locally. At these points,

discontinuities may be observed in the energy spectrum. The discontinuities of $B_n(k)$ are therefore an artefact of wave-turbulence asymptotics, which break down in a small neighbourhood, $k - k_c = O(\varepsilon^2)$, of the critical point.

3 Numerical implementation

For the numerical resolution of Eq. (1), we define a range of modes and wavenumbers. The modes are truncated with $|n| \leq n_{\max}$, $k \leq k_{\max}$. $B_n = B_{-n}$ is used whenever $B_n(k)$ is required for negative n. For each $0 < n \leq n_{\max}$ the set of discretised k consists of exponentially spaced k_i, following

$$k_i = \chi \left(\exp \left[\frac{i}{N} \ln \left(1 + k_{\max}/\chi \right) - 1 \right] \right), \tag{5}$$

where χ is a user specified parameter, comparable to the initial spectral width Ξ. We augmented this set to include also the critical points $k_c \leq k_{\max}$. In what follows, $k_{i,n}$ denotes either a critical value or one of the exponentially spaced wave number values. Critical points k_c are defined by numerical solution of Eqs. (2) and (4).

In time, the numerical solution of the governing Eq. (1) is performed by predictor-corrector scheme. The advantage of this scheme is that due to integrand properties the spectra cannot become negative, therefore satisfying realizability condition. At each half time step the calculation of the nonlinear terms requires the numerical evaluation of the integral over the resonance curve, characterizing interactions bewteen triads of inertial waves. This integral is evaluated using a trapezoidal-style rule. Marching over the resonance curve uses a fourth-order Runge-Kutta integration of the following differential equation:

$$\frac{d\boldsymbol{p}}{ds} = (-Z_2, Z_1), \tag{6}$$

where s is a parameter and $\boldsymbol{Z} = -\nabla_p \sigma$. Because the resonance curve consists of a single loop, it crosses the p_1-axis only in two points $P^- < P^+$. Since it is symmetric about the p_1-axis, calculations are performed from $\boldsymbol{p} = (P^-, 0)$ up to $\boldsymbol{p} = (P^+, 0)$. At each step over the resonance curve, the contributions to the integrals are determined and added into the right-hand-side of Eq. (1).

3.1 Numerical accuracy

The accuracy of the numerical method mainly depends on the numerical resolution in time and in spectral space, namely on the time step and the number of modes and wave-numbers. We characterize it by computing a relative error between each case and a reference case which is the best resolved case that we can afford. The reference case uses $N_t = 256000$, $N_k = 128000$, $n_{\max} = 256$, $k_{\max} = 1.9 \times 10^6$. For all runs, the comparison is done at the fixed time $T = 0.1$, which is the time before which most of the important transient exchanges occur, and after which the spectral evolution corresponds mostly to energy decay.

The computation of the error difference is done by fixing all parameters but one which is varied; namely, for different numbers of time steps N_t (thus corresponding to variations of the timestep itself), for different N_k, characterizing the discretization of the wave-vector k and for different discret modes $n_{\max}$.

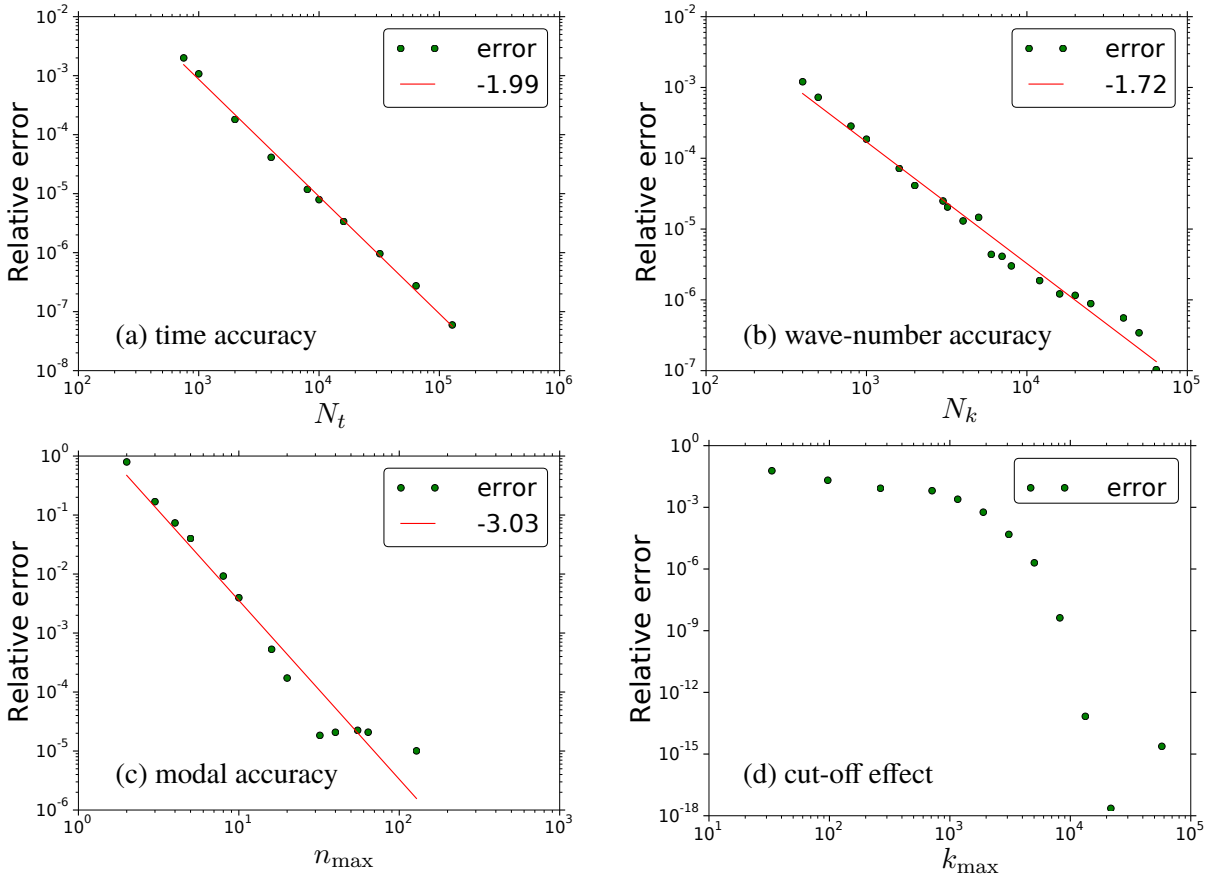

Figure 1: Numerical accuracy and convergence at $T = 0.1$.

For $n_{\max}$ the relative error is defined as

$$\Sigma = \frac{\sum_{k,n} \left| B^{\text{ref}}_{k,n} - B_{k,n} \right|}{\max\limits_{m} \sum_{k} \left| B^{\text{ref}}_{k,m} \right|},$$

and for the other parameters we use

$$\Sigma = \frac{\left\| E^{\text{ref}} - E \right\|_1}{\left\| E^{\text{ref}} \right\|_1},$$

where

$$E(k) = \pi k \sum_{n} B_n(k).$$

As expected, the predictor-corrector scheme is of second-order in time (Fig. 1a) and the method is convergent in the spectral space: the convergence curves show a -1.7 accuracy in wave-number and -3 in the modal representation (Figs. 1b and c). In addition, the influence of the cut-off effect is shown in Fig. 1d: increasing the maximal value of k, $k_{\max}$, by adding the required number of points, a rapid decline through the dissipative range is observed, meaning that, for the case shown in Fig.1d, $k_{\max} \simeq 10^4$ is enough for adequate resolution in the small wavenumbers range, and there is no need to increase its value.

All these results allow to choose a set of numerical parameters providing adequate accuracy for a given

set of physical parameters.

3.2 Numerical efficiency

In order to decrease the computational walltime, the method has been parallelized to distribute the integrations over the resonance curves between different processors. Communications are performed by the MPI library. This allows to obtain a good speedup up to 128 processes and more than 86% of efficiency (Fig. 2, 100% corresponding to the ideal speed-up); which is rather good compared with the efficiency of standard Navier-Stokes Eulerian solvers or pseudo-spectral methods for Direct Numerical Simulations.

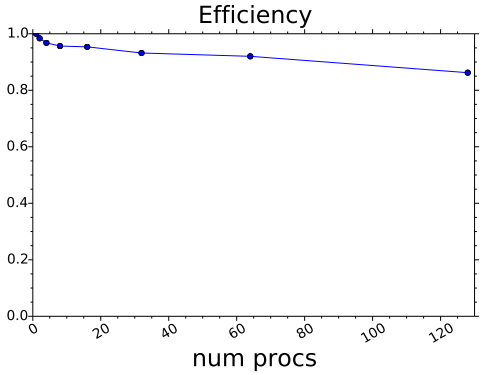

Figure 2: Efficiency of the numerical scheme for the wave turbulence model, computed as the ratio of the time spent by several processes to the time for one process computation divided by the number of processes.

4 Results

4.1 Conservation of the wave-component energy

The wave turbulence model is supposed to conserve the energy of the $n \neq 0$ modes. It can be verified numerically in the inviscid case. With zero viscosity, the energy can only be redistributed over all the scales that leads to an equipartition of the energy for long enough time. This is known as the thermalization mechanism in statistical mechanics. This has been reproduced numerically, as illustrated in the Fig. 3. The energy is first accumulated in the small scales, near the cut-off and this saturation process successively propagates backwards to larger scales, eventually leading to the expected equipartition of energy. The fact that our numerical scheme is able to capture this pile-up of energy in the small scales without blowing out is a good indicator of its robustness.

4.2 Spectral evolution

The initial form of the energy spectrum corresponding to Eq. (3) and the spectral density of the first ($n = 1$) and second modes ($n = 2$) are given in Fig. 4a. As time evolves, the energy is transferred towards smaller scales (Fig. 4b). Once the energy has been transferred to sufficiently small scales, the dissipation rate becomes strong enough to balance the incoming energy. Thus, equilibrium is established and an inertial regime is reached due to the cascade by nonlinear interactions into higher wavenumbers (Fig. 4c). For larger times, the spectrum decays due to viscous effect (Fig. 4d).

During the evolution, the system encounters a critical time $T \simeq 0.0648$ which corresponds to the passage

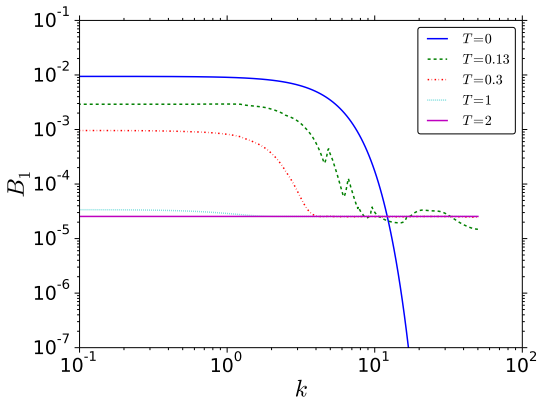

Figure 3: Thermalization mechanism.

through a dynamical singularity. Capturing this phase is numerically demanding, all the more at small viscosity, but it cannot be avoided since one wishes to obtain the long time spectral evolution.

Behaviour at critical points For a given set of numerical and physical parameters, the critical points locations could be found numerically. The discontinuities, which they imply in the modes, has been observed in the zoomed area of Fig. 4c.

Full spectral distribution The spectral distribution of energy over the wavenumbers k and modes n in Fig. 5 shows that the cascade of energy occurs mainly in the wavenumber space and much less between modes (in the wall-normal direction), supporting the fact that major mechanisms occurs in planes parallel to the wall.

4.3 Influence of wall and volumetric damping

The damping factor $\Delta_n(k)$ can be written as

$$2\varepsilon^{-2} Re(\Delta_n(k)) = f_w + f_v, \tag{7}$$

where

$$f_w = \beta_w \frac{(1-\omega_n^2(k))^{1/2}}{\sqrt{2}} \left\{ (1+\omega_n(k))^{3/2} + (1-\omega_n(k))^{3/2} \right\}, \qquad f_v = \beta_v (k^2 + n^2\pi^2)$$

and $\beta_w = 2\varepsilon^{-2}E^{1/2}$ and $\beta_v = 2\varepsilon^{-2}E$ are parameters measuring the importance of wall and volumetric damping. Therefore, viscous dissipation can be computed as

$$\epsilon(t) = \sum_{n=1}^{\infty} \int_0^{\infty} \pi f k B_n(k,t) \mathrm{d}t$$

for each contribution by selecting $f = f_w$ and $f = f_v$ for wall and volumetric damping respectively. Since the Ekman number E is small, $\beta_v \ll \beta_w$ and wall damping generally dominates at large scales. However, volumetric damping becomes significant if $k^{-1}(k^2 + n^2\pi^2)^{3/2}$ is of order $E^{1/2}$.

Looking at the time evolution of the dissipation in Fig. 6-right, it can be seen that, at short time and

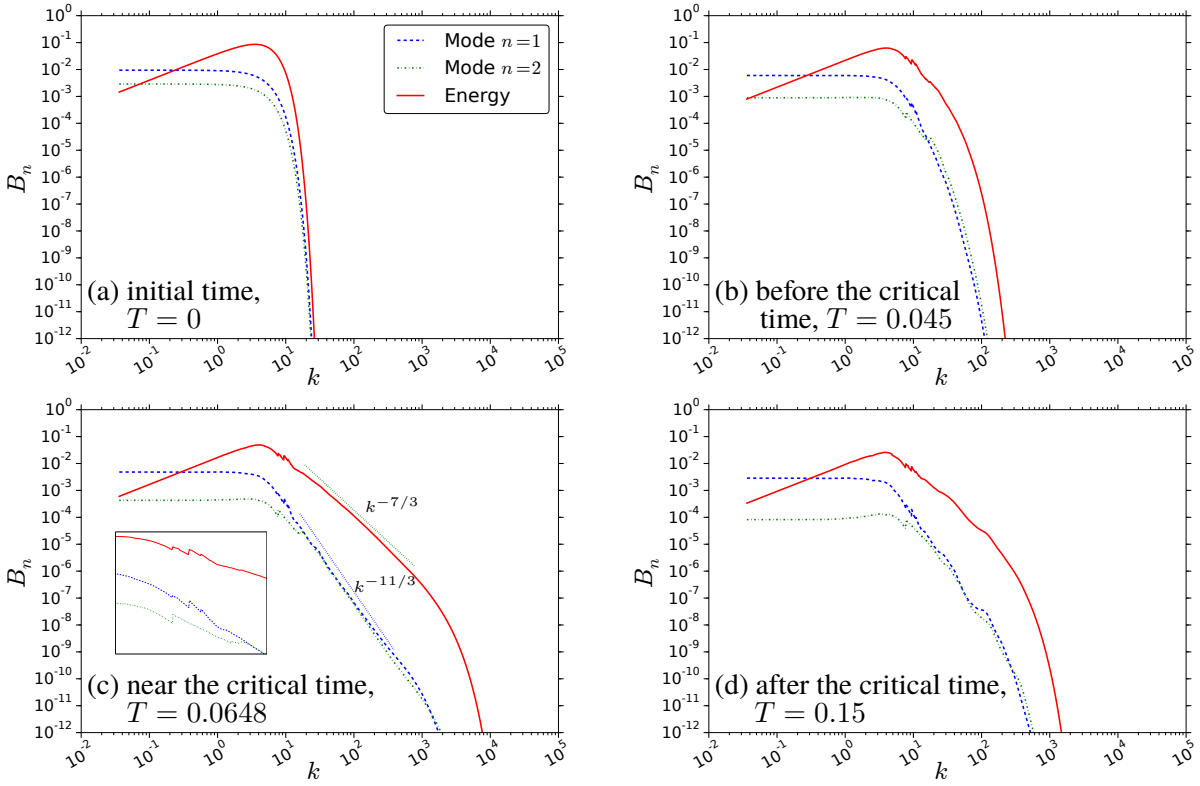

Figure 4: Spectral evolution at different stages, starting from the initial condition, going through the critical time, and reaching the viscous decay regime, from (a) to (d) (non dimensional times are indicated on each plot). Panel (c) also shows a zoom of the spectral region containing critical points.

for this choice of physical parameters, the dissipation coming from the walls is initially larger than volumetric dissipation. However, the latter increases dramatically when the front of the spectrum at small scales reaches the dissipative scale, due to the nonlinear cascade of energy. At the critical time, the spectrum has reached its full spectral extent and volumetric dissipation becomes larger than wall dissipation. After $T \simeq 0.065$, viscous decay begins and eventually the volumetric dissipation becomes of the same order or smaller than wall dissipation which in the meantime has not decreased as much. Looking at the energy evolution in Fig-6-right, at short time the energy remains almost constant (or decays slightly if wall damping parameter β_w is not very small), but when the fluid motion occupies the full spectral extension in the large wavenumbers energy, and populates the very small scales, energy decays exponentially.

5 Conclusion

We have considered the wave-turbulence closure proposed by Scott (2014) [6] for studying the dynamics of rapidly rotating, decaying turbulence confined in a single direction of the rotation. We have proposed a numerical implementation of this model, and obtained an efficient code which is suitable for running the numerous cases required for a complete parametric study. This has gone through the parallelization of the code, whose speed-up efficiency is very good.

We have begun by varying the numerical parameters of the model in order to evaluate the properties of the complex numerical scheme. This study first demonstrates the convergence of the model with respect

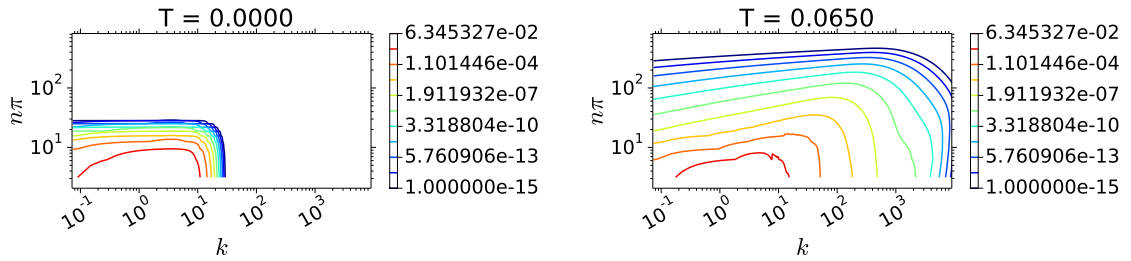

Figure 5: Energy contours at initial time (on the left) and immediately after the critical time (on the right).

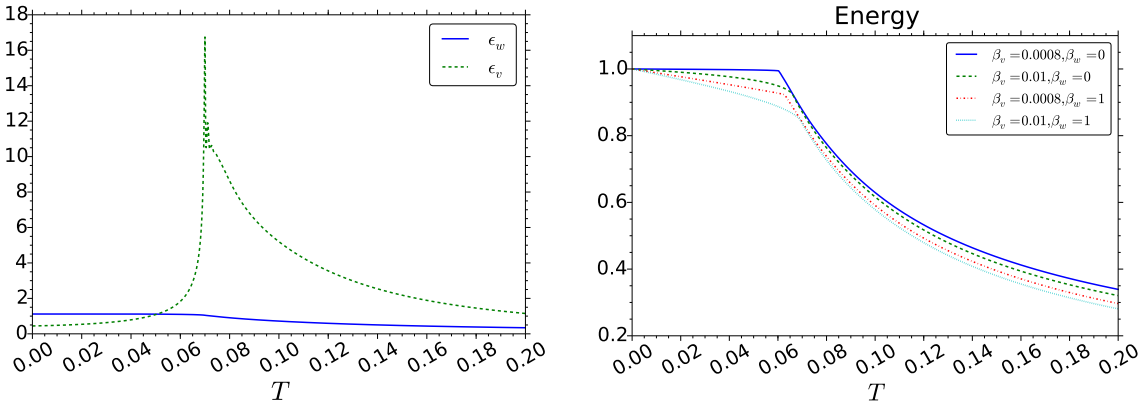

Figure 6: Left: Wall damping ϵ_w and volumetric viscous dissipation ϵ_v. Right: Total energy time evolution.

to all the numerical parameters. Second, this study permits to extrapolate the required accuracy, in terms of number of modes and wavenumbers, as well as timestep, necessary for representing reliable physical mechanisms. We thus have had to deal with the presence of critical points in the spectrum and with a critical time inherent to the nature of the dynamical system. Thirdly, when studying the conservation property of the model in an inviscid case, we have observed the appearance of an asymptotic thermalized state consistent with predictions of statistical mechanics, and confirming the robustness of the numerics.

We then studied the statistics produced by the model for an initial set of physical parameters. The artifact of the wave-turbulence approach manifests in the form of discontinuities of the spectra and is explained by the presence of critical points predicted by the theory when considering the resonant curves in spectral space associated with resonant triads We have observed that, for our choice of viscosity and wall damping parameter, dissipation in the wall region dominates up to a certain time. After that time, the small dissipative scales have received enough energy to become the main source of dissipation, and volumetric damping dominates and produce an exponential decay of total kinetic energy.

Now that this preliminary study is completed, in future work we will concentrate on exploring all the possible dynamics that are permitted by the wave-turbulence model, by extending the range of physical parameters and choosing different initial conditions.

References

[1] G.K. Batchelor. *The theory of homogeneous turbulence*. Cambridge University Press, 1953.

[2] F. Bellet, F.S. Godeferd, J.F. Scott, and C. Cambon. Wave turbulence in rapidly rotating flows. *Journal of Fluid Mechanics*, 562:83–121, 2006.

[3] C. Cambon and L. Jacquin. Spectral approach to non-isotropic turbulence subjected to rotation. *Journal of Fluid Mechanics*, 202:295–317, 1989.

[4] C. Cambon, N.N Mansour, and F.S. Godeferd. Energy transfer in rotating turbulence. *Journal of Fluid Mechanics*, 337:302–332, 1997.

[5] A.C. Newell and B. Rumpf. Wave turbulence. *Ann. Rev. Fluid Mech.*, 43:59–78, 2011.

[6] J.F. Scott. Wave turbulence in a rotating channel. *Journal of Fluid Mechanics*, 741:316–349, 2014.